Isobaric Analog Resonances in Proton Inelastic Scattering from ^{136}Xe†

P. A. MOORE* AND P. J. RILEY*
University of Texas, Austin, Texas 78712
AND
C. M. JONES AND M. D. MANCUSI‡
Oak Ridge National Laboratory, Oak Ridge, Tennessee 37830
AND
J. L. FOSTER, JR.§
University of Pittsburgh, Pittsburgh, Pennsylvania 15213
(Received 24 October 1969)

Thirty-six excited states of ^{136}Xe at excitation energies up to 6.3 MeV have been observed in proton inelastic-scattering excitation-function measurements at proton energies from 9.77 to 12.89 MeV. The 2^+ first excited state at 1.30 MeV and the second excited state at 1.68 MeV resonate strongly at all of the lowest isobaric analog resonances, indicative of a collective nature for these states. Excitation functions for many of the remaining states exhibit resonant behavior characteristic of neutron-particle–neutron-hole excited states. Proton inelastic angular distributions have been measured at the lowest five analog resonances. Angular distributions for the particle-hole states at the first ($f_{7/2}$), second ($p_{3/2}$), and fourth ($f_{5/2}$) analog resonances have been fitted to determine the hole structure of the particle-hole configurations. Using the results of this analysis in conjunction with the resonant behavior of the corresponding inelastic excitation functions, it has been possible to determine particle-hole configurations and spin assignments for a number of excited states of ^{135}Xe.

I. INTRODUCTION

THE study of isobaric analog resonances has been shown to provide a useful tool for the determination of nuclear structure in heavy nuclei. Most recently, these studies have dealt with resonant inelastic scattering, and measurements on a number of targets[1–6] have demonstrated the usefulness of these observations in determining the structure of excited states of the target nucleus.

We have recently completed an extensive series of measurements of elastic and inelastic proton scattering from the closed $N=82$ neutron shell nucleus ^{136}Xe in the bombarding energy region from 9.77 to 12.98 MeV. Analysis of the proton elastic excitation functions[7] has shown that well-defined isobaric analog resonances occur at laboratory bombarding energies of 10.270 ($f_{7/2}$), 10.874 ($p_{3/2}$), 11.255 ($p_{1/2}$), 11.583 ($f_{5/2}$), and 11.810 ($f_{5/2}$) MeV, and that the corresponding compound-nuclear states in ^{137}Cs are analogs of states in ^{137}Xe formed by the addition of a neutron to the closed $N=82$ neutron shell in the configurations indicated above. Virtually all of the proton inelastic excitation functions show resonant structure at these same resonances, or at higher resonances observed in the elastic scattering data. Many of these excitation functions have an even more distinctive behavior in that they exhibit sharp peaks at only a very few of the analog resonances. In agreement with measurements of a similar nature on other heavy nuclei,[3,4,6,8] these inelastic transitions can be identified as being due to the excitation of neutron-particle–neutron-hole excited states in ^{136}Xe. In the present work, we have analyzed these data in conjunction with a simple theory to extract quantitative information about the spins, parities, and particle-hole configurations of the residual particle-hole states.

II. EXPERIMENTAL PROCEDURE

The incident proton beam was obtained from the Oak Ridge National Laboratory EN Tandem Van de Graaff accelerator. The target gas was contained within a 3-in.-diam gas cell used in conjunction with the ORNL precision gaseous target scattering chamber.[9] Beam entrance and exit windows were 25-μ in.-thick nickel foils. The cell walls were 0.00025-in.-thick alumi-

† Research participation at Oak Ridge sponsored by Oak Ridge Associated Universities.
* Research sponsored by the U.S. Atomic Energy Commission under contract with Union Carbide Corporation.
‡ U.S. Atomic Energy Commission Postdoctoral Fellow under appointment from the Oak Ridge Associated Universities. Present address: Bell Telephone Laboratories, Holmdel, N.J.
§ Present address: Université de Montréal, Montreal, Canada.
[1] E. W. Hamburger, J. Kremenek, B. L. Cohen, J. B. Moorhead, and C. Shin, Phys. Rev. **162,** 1158 (1967).
[2] E. J. Schneid, E. W. Hamburger, and B. L. Cohen, Phys. Rev. **161,** 1208 (1967).
[3] C. F. Moore, J. G. Kulleck, P. von Brentano, and F. Rickey, Phys. Rev. **164,** 1559 (1967).
[4] G. C. Morrison, N. Williams, J. A. Nolen, Jr., and D. van Ehrenstein, Phys. Rev. Letters **19,** 592 (1967).
[5] J. L. Roster, O. Dietzsch, and K. Schechet, Bull. Am. Phys. Soc. **13,** 70 (1968).
[6] J. P. Wurm, A. Henslee, and P. von Brentano, Nucl. Phys. **A128,** 433 (1969).
[7] P. A. Moore, P. J. Riley, C. M. Jones, M. D. Mancusi, and J. L. Foster, Phys. Rev. **180,** 1213 (1969).
[8] S. A. A. Zaidi, J. L. Parish, J. G. Kulleck, C. F. Moore, and P. von Brentano, Phys. Rev. **165,** 1312 (1968).
[9] C. M. Jones, J. W. Johnson, and R. M. Beckers, Nucl. Instr. Methods **68,** 77 (1969).

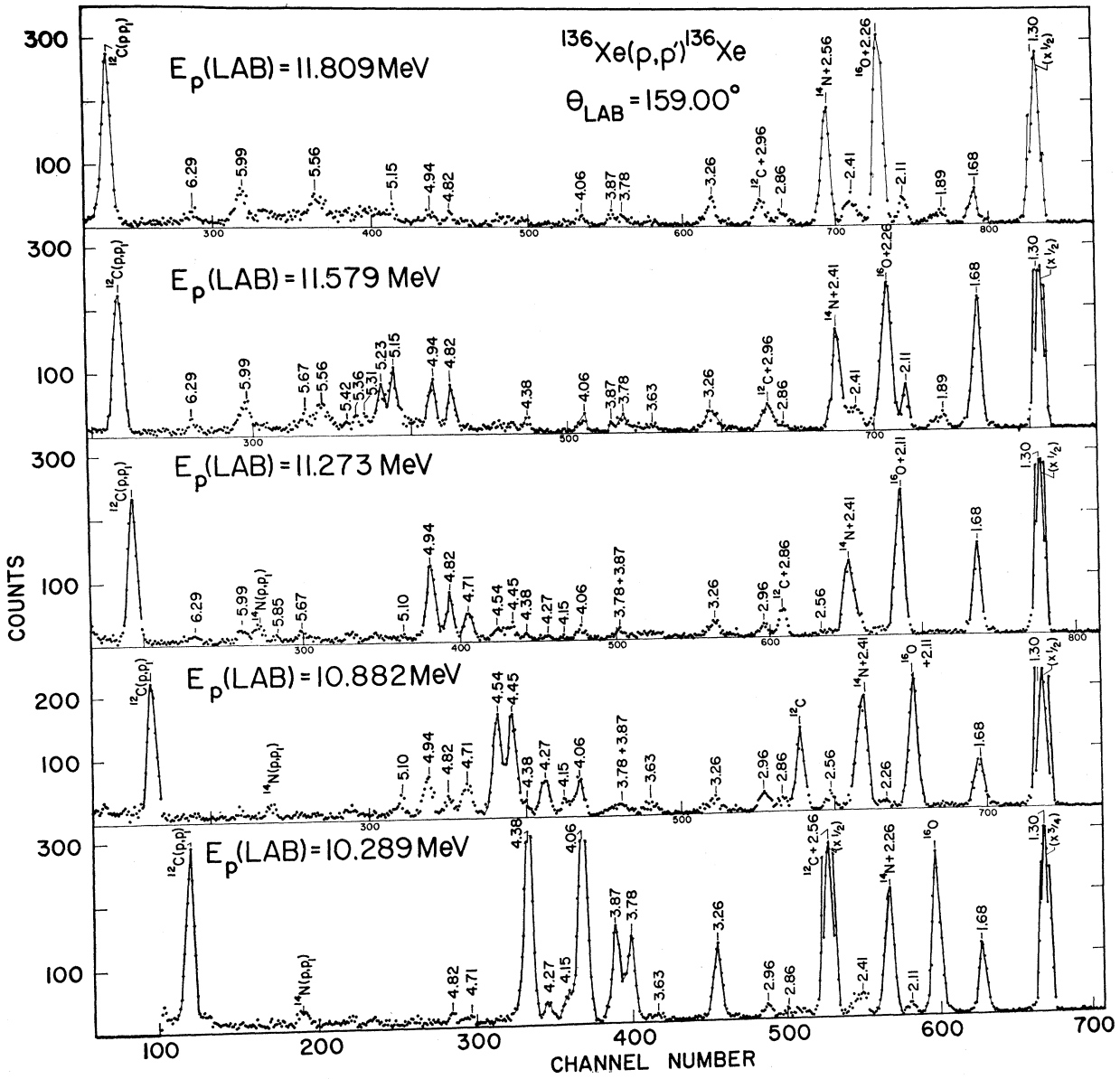

FIG. 1. Pulse-height spectra for the inelastic scattering of protons from ^{136}Xe at a scattering angle of 159.00°, measured in the vicinity of the $f_{7/2}$, $p_{3/2}$, $p_{1/2}$, $f_{5/2}$, and $f_{5/2}$ analog resonances at laboratory proton energies of 10.289, 10.882, 11.273, 11.579, and 11.809 MeV, respectively. The excitation energies of states observed in ^{136}Xe are indicated.

nized Mylar. The beam current used was typically 0.3 μA, and the total charge collection at each energy was approximately 400 μC. The gas pressure was typically 0.068 atm, corresponding to a target thickness of approximately (250/sinθ_{lab}) μ_g/cm^2. Four 2-mm-thick lithium-drifted silicon detectors, cooled to dry-ice temperature, were used.

Pulse-height spectra, measured in the vicinity of the $f_{7/2}$, $p_{3/2}$, $p_{1/2}$, $f_{5/2}$, and $f_{5/2}$ analog resonances at laboratory proton energies of 10.289, 10.882, 11.273, 11.579, and 11.809 MeV, respectively, are shown in Fig. 1. An additional spectrum, measured at a laboratory proton energy of 11.530 MeV, is shown in Fig. 2. This spectrum shows more clearly the states at excitations between 5.85 and 6.29 MeV. Two additional states, at excitations of 3.16 and 3.31 MeV, are also resolved in this spectrum. The laboratory angle for all spectra in these figures is 159.00°, and in each case the elastic peak has been omitted in the plot. The over-all experimental resolution was 50 keV.

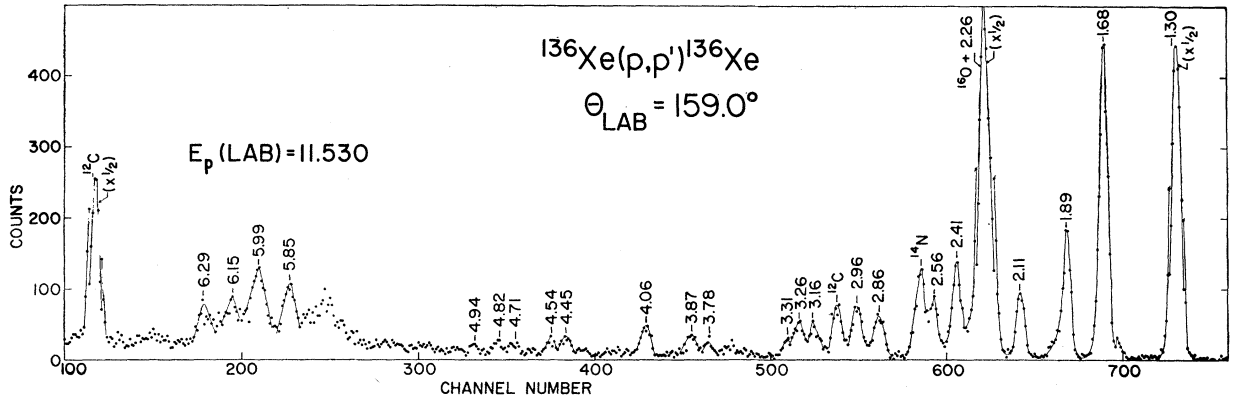

FIG. 2. Pulse-height spectrum for the inelastic scattering of protons from ^{136}Xe at a scattering angle of 159.00° and a laboratory proton energy of 11.530 MeV. This spectrum shows more clearly the states at excitations between 5.85 and 6.29 MeV. Two additional states, at 3.16 and 3.31 MeV, are also resolved in this spectrum.

III. ENERGY LEVELS OF ^{136}Xe

Proton groups leading to 36 excited states of ^{136}Xe are discernible in the spectra. An energy level diagram for the observed states in ^{136}Xe is shown in Fig. 3. Spin assignments for many of the levels are included in the figure with parentheses indicating those which are tentative. The means by which these assignments were made will be discussed later.

Q values for the observed inelastic transitions were deduced as follows: Each pulse-height spectrum contained five peaks resulting from reactions of known Q value [^{136}Xe, ^{12}C, ^{14}N, ^{16}O elastic scattering, and $^{12}C(p, p_1)$ inelastic scattering]. These peaks spanned the entire spectrum of $^{136}Xe(p, p')$ groups. A least-squares-fitting code calculated kinematically the energy of each peak of known Q value for each spectrum and made both a linear and a quadratic least-squares fit to these points to determine energy versus channel number for all channels. Then, given the channel number of any other proton group in the spectrum, its energy could be determined and its Q value calculated. Due to the large energy range spanned by the peaks used for the least-squares fit, the quadratic fit was found in this case to give the best over-all consistency for Q values of a given group, indicating a possible slight nonlinearity in the electronics. This procedure was applied to spectra measured at 90° and 159°. The runs chosen were the five runs on each side of the first four resonances in the elastic excitation functions, resulting in a Q-value calculation for a maximum of 80 spectra for a given group, assuming that the group was visible in all 80 spectra. The results were checked for consistency between the spectra and averaged to give Q values for the 36 proton groups discernible in the various spectra. A maximum absolute uncertainty of about ± 20 keV is assigned to these Q values, with a much smaller relative uncertainty. As pointed out by Wurm *et al.*[6] an important question concerns the identity of closely spaced levels apparently populated by more than one resonance. Since in the present work complete excitation functions were measured, and the background was sufficiently low that most levels were observed at all energies above the energy where they first became visible, it is felt that a high degree of reliability can be placed on the present identification of levels.

IV. CROSS-SECTION DATA

The inelastic-scattering data consist of inelastic proton excitation functions and angular distributions for the various group. Xenon gas, isotopically enriched to 91% ^{136}Xe and 8% ^{134}Xe, was used in most of these measurements. However, angular distributions at the first three analog resonances were measured using xenon gas enriched to 95% ^{136}Xe. All cross sections shown were corrected for the isotopic concentration of ^{136}Xe.

Figure 4 shows excitation functions for all of the inelastic proton groups discernible in the spectra except those at excitations of 3.16 and 3.31 MeV, which were unresolved in nearly all of the spectra. The arrows indicate the location of resonances in the elastic scattering analysis.[7] Initially, inelastic excitation functions were measured for proton energies between 9.77 and 12.54 MeV (region I) at laboratory angles of 159.00°, 146.25°, 123.75°, and 90.00°. Later these measurements were extended from 12.10 to 12.98 MeV (region II) for the 159.00° data. The resonant behavior of the region-I excitation functions was found to be the same at all four angles for all states except those with excitations between 5.23 and 5.67 MeV. These states were more clearly resolved at 146.25° than at 159.00°, and exhibited resonant behavior at 146.25° not observed in the 159° data. Therefore, the 146.25° data, rather than the 159° data, is shown in Fig. 4(e) for these states. In addition, due to the presence of carbon, oxygen, and nitrogen contaminants in the spectra, the groups at excitation between 2.11 and 2.96 MeV remained uncontaminated only at 90° for the entire

energy range. The 90° excitation function for these groups suffered, however, from poor counting statistics as a result of the decreased effective target length. Therefore, it was necessary to piece together excitation functions for these groups [see Fig. 4(b)] from the data at 159.00°, 146.25°, and 123.75° in order to determine their resonant behavior. Gaps in the excitation functions for these and other proton groups shown in the figure indicate either that the peak was contaminated or that it was undiscernible in the spectra corresponding to that energy range. Finally, the groups at excitations of 3.78 and 3.87 MeV were not resolved past the first analog resonance, and therefore an additional excitation function, representing the yield from both these groups, is shown in Fig. 4(a).

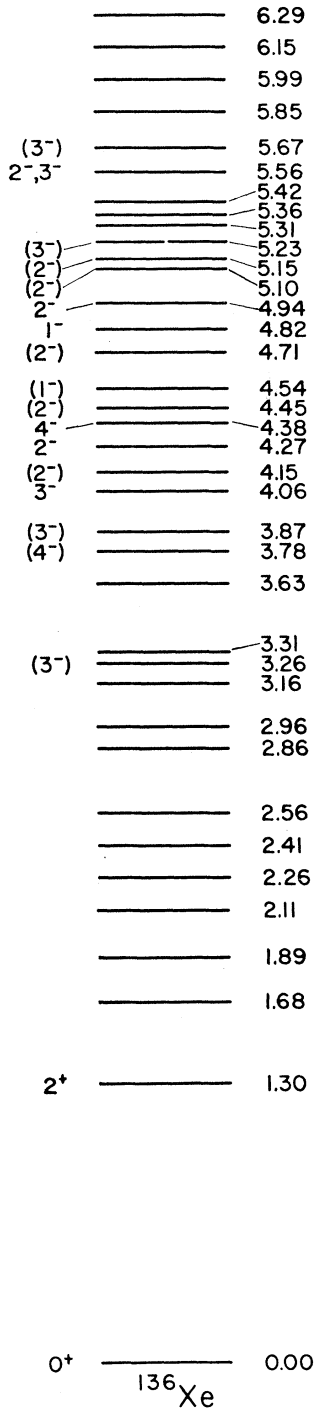

FIG. 3. An energy level diagram for states of ^{136}Xe observed in this experiment. Spin assignments and excitation energies are indicated. Parentheses indicate tentative spin assignments.

Proton inelastic angular distributions were measured near the $f_{7/2}$, $p_{3/2}$, $p_{1/2}$, $f_{5/2}$, and $f_{5/2}$ analog resonances at laboratory proton energies of 10.261, 10.869, 11.266, 11.570, and 11.820 MeV, respectively. In addition, one off-resonance angular distribution was measured at a laboratory energy of 10.642 MeV (between the $f_{7/2}$ and $p_{3/2}$ resonances). These data are shown in Figs. 5–7.

V. RESULTS AND DISCUSSION

A. General Discussion

As can be seen from Fig. 4, all the low-lying inelastic states in ^{136}Xe below 3-MeV excitation exhibit a rather complex resonant behavior indicating that these states are either collective in nature, or that they have a rather complicated shell-model character. On the other hand, most of the states above 3-MeV excitation resonate at most at only a few of the analog resonances, indicating what is probably neutron particle-hole structure. Virtually all of the low-lying inelastic states resonate at the ground-state $f_{7/2}$ analog resonance, and at the first excited $p_{3/2}$ analog resonance. The only inelastic resonant behavior observed at the $h_{9/2}$ analog resonance are weak resonances in the yields to the 5.23-, 5.31-, 5.36-, 5.42-, and 5.56-MeV levels. The resonant behavior becomes more complex at proton energies above 12 MeV, where resonant behavior in the yields of the lowest three excited states at 1.30, 1.68, and 1.86 MeV dies out, while the more highly excited of the low-lying states (below 3-MeV excitation), and the more highly excited of the "particle-hole" states exhibit strongly resonant behavior.

It has been pointed out by Cosman *et al.*[10] that several effects can cause enhancement of an inelastic transition at an incident proton energy corresponding to an analog state in the compound system. Consider, for example, the transition to the first ^{136}Xe state [denoted by (2_1^+)] from the ^{137}Xe ground-state analog with $J^\pi = 7/2^-$ at $E_p = 10.270$ MeV. Since the $f_{7/2}^-$ neutron spectroscopic factor for the ^{137}Xe ground state is 0.74,[11] much of the remaining fraction of the wave function may be built from a neutron coupled to the 2_1^+ state to give $J^\pi = \frac{7}{2}^-$. Following Cosman *et al.*, the analog-

[10] E. R. Cosman, J. M. Joyce, and S. M. Shaforth, Nucl. Phys. **A108**, 519 (1968).

[11] P. A. Moore, P. J. Riley, C. M. Jones, M. D. Mancusi, and J. L. Foster, Phys. Rev. **175**, 1516 (1968).

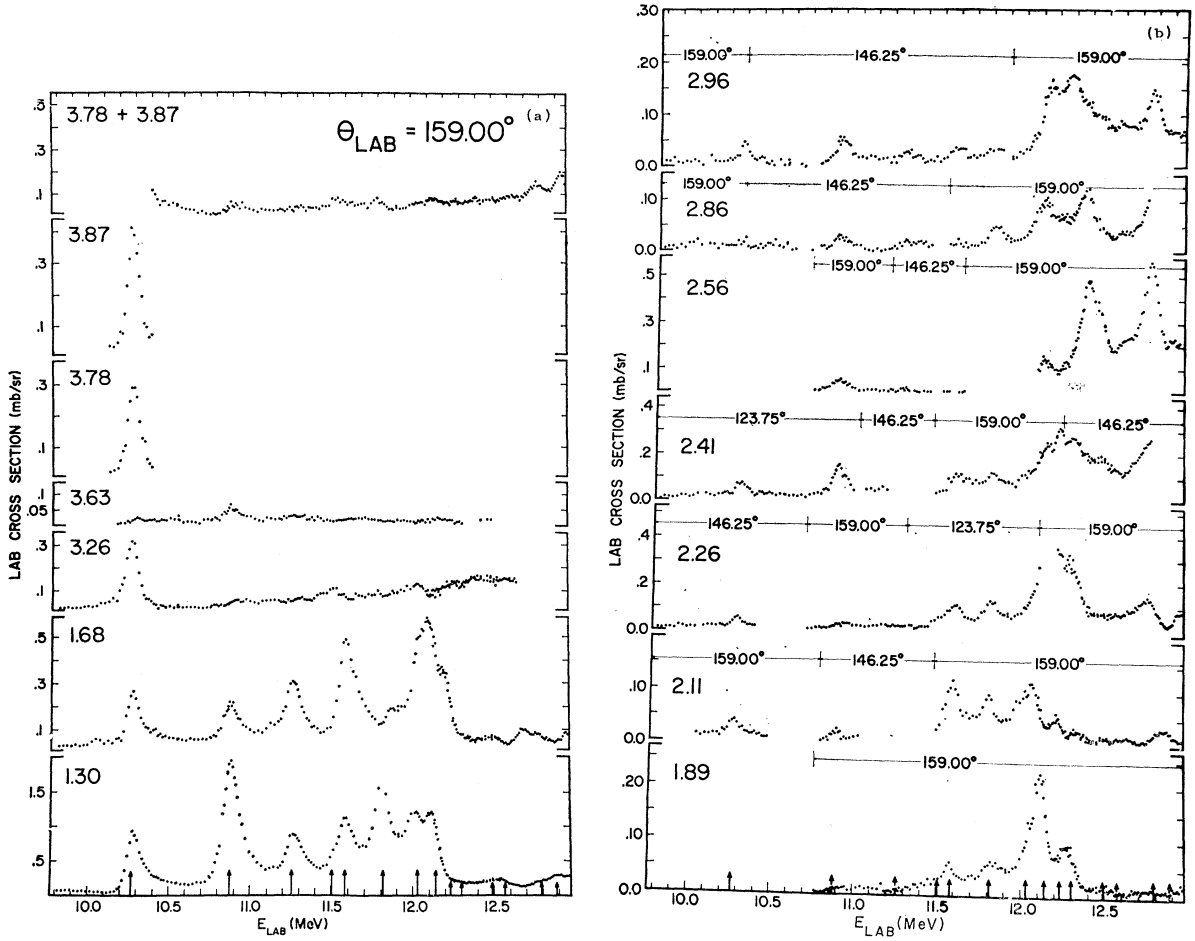

FIG. 4. Inelastic excitation functions for the scattering of protons from ^{136}Xe. Excitation energies of the residual states in ^{136}Xe are indicated. Arrows indicate the location of resonances in the elastic scattering analysis at the following energies: 10.270 ($f_{7/2}$), 10.874 ($p_{3/2}$), 11.255 ($p_{1/2}$), 11.505 ($h_{9/2}$), 11.583 ($f_{5/2}$), 11.810 ($f_{5/2}$), 12.028 ($f_{5/2}$), 12.138 ($p_{3/2}$), 12.229 ($p_{1/2}$), 12.299 ($f_{5/2}$), 12.490 ($p_{1/2}$) 12.571 ($f_{5/2}$), 12.791 ($p_{3/2}$), and 12.882 MeV ($p_{1/2}$). In Fig. 4(b), excitation functions for the groups between 2.11 and 2.96 MeV were pieced together from the 159.00°, 146.25°, and 123.75° data in order to determine their resonant behavior.

state wave function may be written as

$$\psi_0{}^A=[1/(2T_0+1)^{1/2}][T^-\{\alpha(f_{7/2})_n\psi_0\}+T^-\{\beta(l_j)_n\psi_{2^+}\}_{7/2^-}+\cdots],$$

where ψ_0 and ψ_{2^+} are wave functions of the ground and first 2^+ states in ^{136}Xe, $|\alpha|^2=0.74$, and $T^-=\sum_i t_i^-$, where t_i^- is the isospin lowering operator for ith particle. Values of $l=1$ and $l=3$, with j^π values of $\frac{3}{2}^-$, $\frac{5}{2}^-$, and $\frac{7}{2}^-$ are expected to contribute to the second term. We can expand $\psi_0{}^A$ as follows:

$$\begin{aligned}\psi_0{}^A&=(1/\sqrt{29})[\alpha(f_{7/2})_p\psi_0+\alpha(f_{7/2})_nT^-\psi_0+\beta\{(l_j)_p\psi_{2^+}\}_{7/2^-}+\beta\{(l_j)_nT^-\psi_{2^+}\}_{7/2^-}]\\&=(1/\sqrt{29})[\alpha(f_{7/2})_p\psi_0+\{\alpha\sqrt{2}(f_{7/2})_n(s_{1/2},s_{1/2}{}^{-1})\psi_0+\alpha(\sqrt{4})(f_{7/2})_n(d_{3/2},d_{3/2}{}^{-1})\psi_0+\cdots\}\\&\quad+\beta\{(l_j)_p\psi_{2^+}\}_{7/2^-}+\beta\sqrt{2}\{(l_j)_n(s_{1/2},s_{1/2}{}^{-1})\psi_{2^+}\}_{7/2^-}+\beta(\sqrt{4})\{(l_j)_n(d_{3/2},d_{3/2}{}^{-1})\psi_{2^+}\}_{7/2^+}+\cdots],\end{aligned}$$

where (l_j, l_j^{-1}) is an operator which creates a proton-particle–neutron-hole pair, each with angular momentum l_j, coupled to give total $J=0$. We have explicitly included $s_{1/2}$ and $d_{3/2}$ particle-holes because these levels are closest to the Fermi surface in the $N=82$ closed shell.

The elastic channel is strongly coupled to $\psi_0{}^A$ through the first term in the equation; similarly, the p', $2_1{}^+$ channel is strongly coupled to $\psi_0{}^A$ through the term $\beta\{(l_j)_p\psi_{2^+}\}_{7/2^-}$. In addition to this process, which has been designated process I by Cosman *et al.*, there could in principle be good overlap of p', $2_1{}^+$ with other terms in the equation. That is, if 1-particle–1-hole terms of the type $\{(f_{7/2})_n\ (d_{3/2})_n{}^{-1}\psi_0\}_{2^+}$ were present in the $2_1{}^+$ wave function, a decay in the p', $2_1{}^+$ channel could be favored by emission of the $d_{3/2}$ proton. However, in the present case, terms of this type, called process II, are parity forbidden, and should not be observed in proton decay to positive-parity states. Process-II decays to particle-hole states are, of course, anticipated.

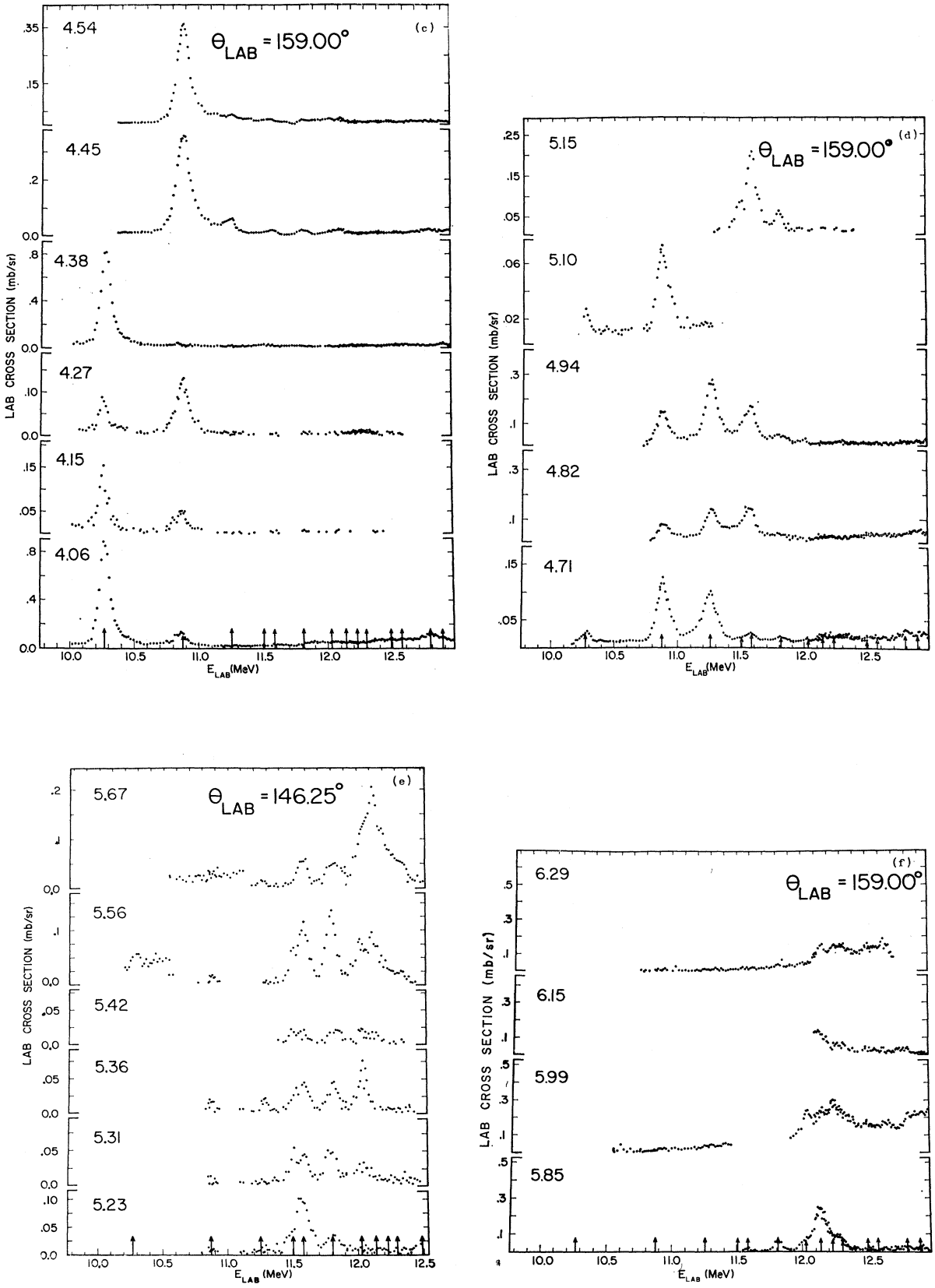

FIG. 4. (*Continued*).

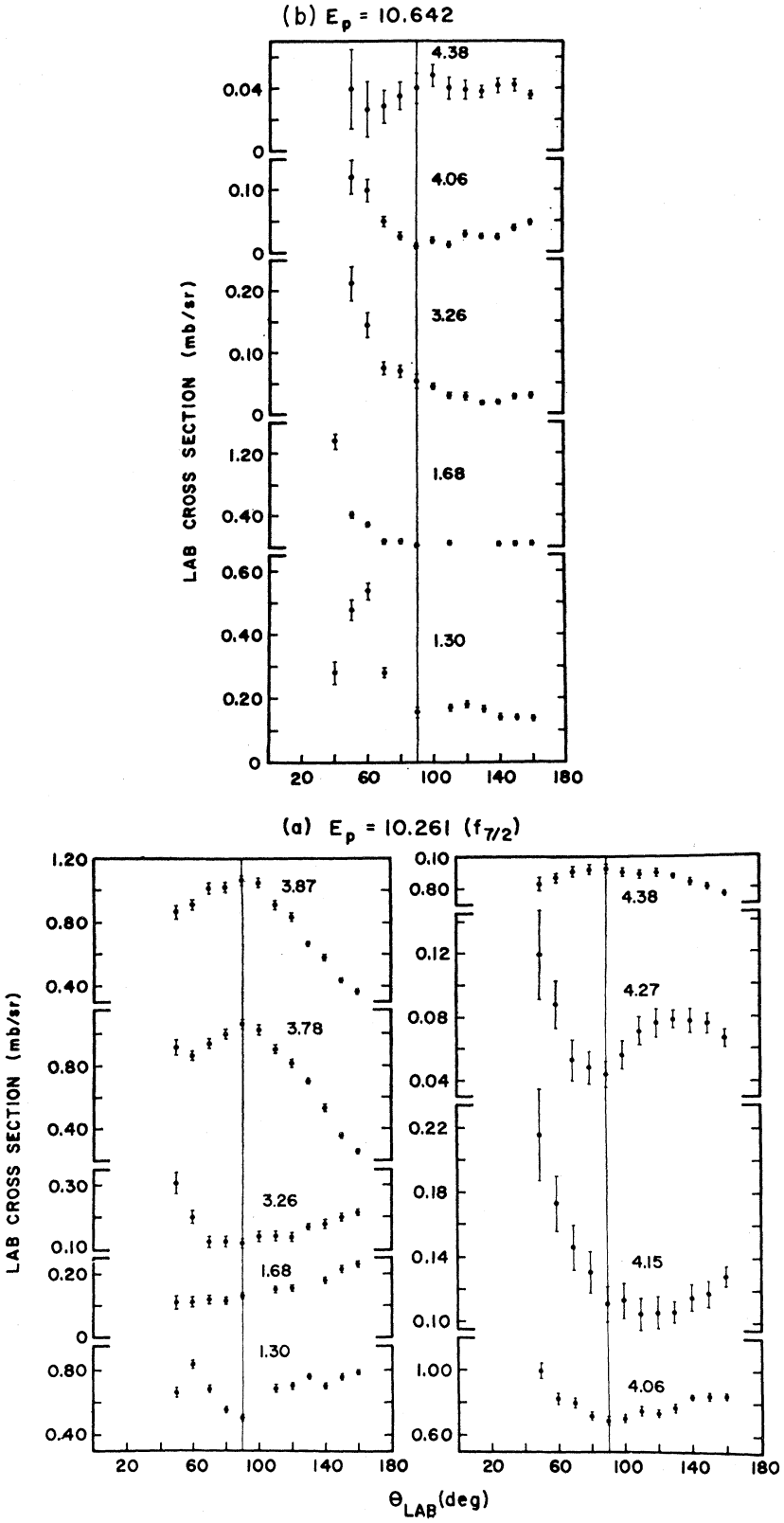

FIG 5. Inelastic angular distributions for the scattering of protons from ^{136}Xe measured near the $f_{7/2}$ analog resonance (a), and at an off-resonance proton energy of 10.642 MeV (b). Error bars indicate the statistical uncertainty in the measurements.

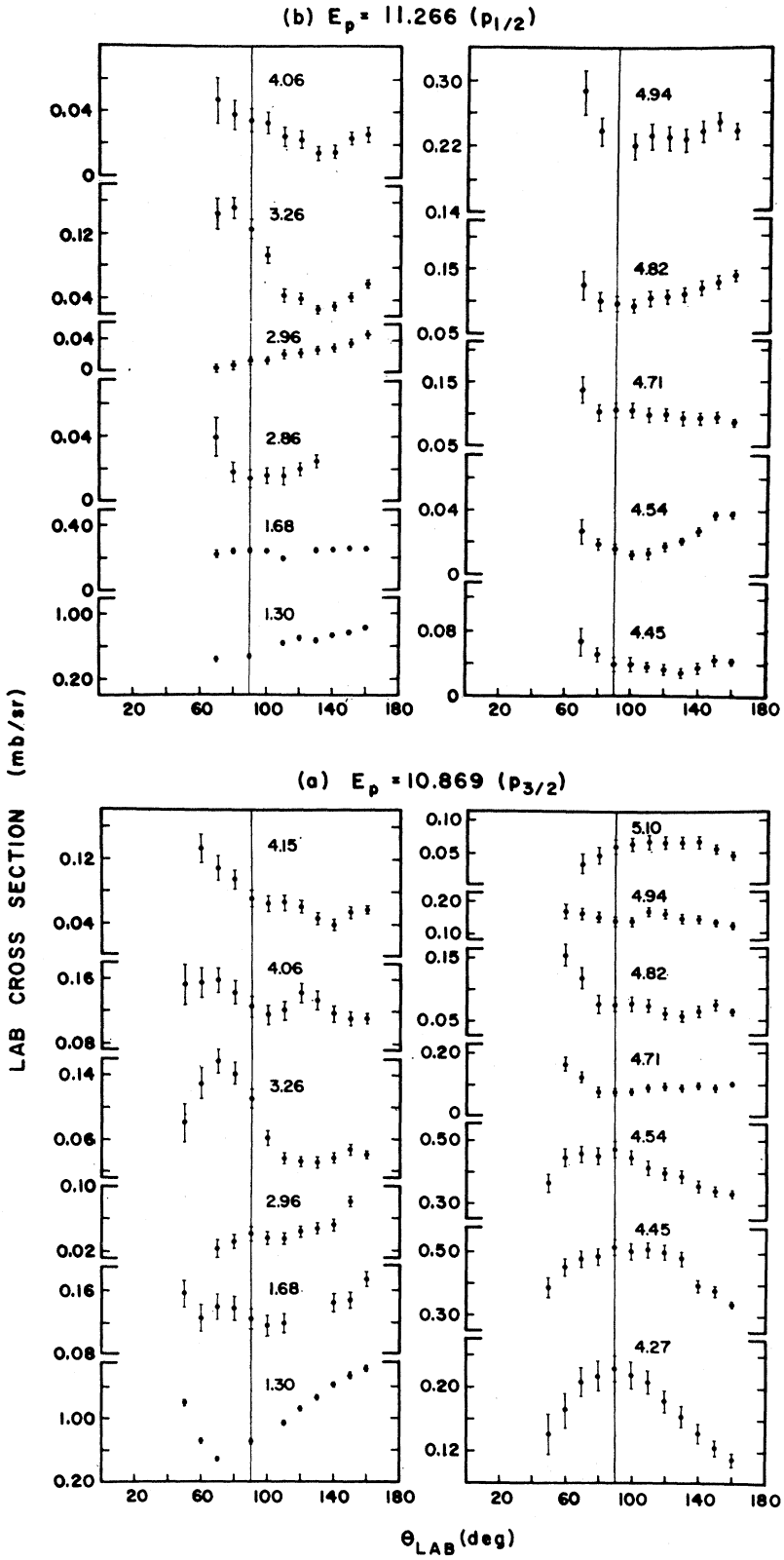

FIG. 6. Inelastic angular distributions for the scattering of protons from ^{136}Xe measured near the (a) $p_{3/2}$ and (b) $p_{1/2}$ analog resonances.

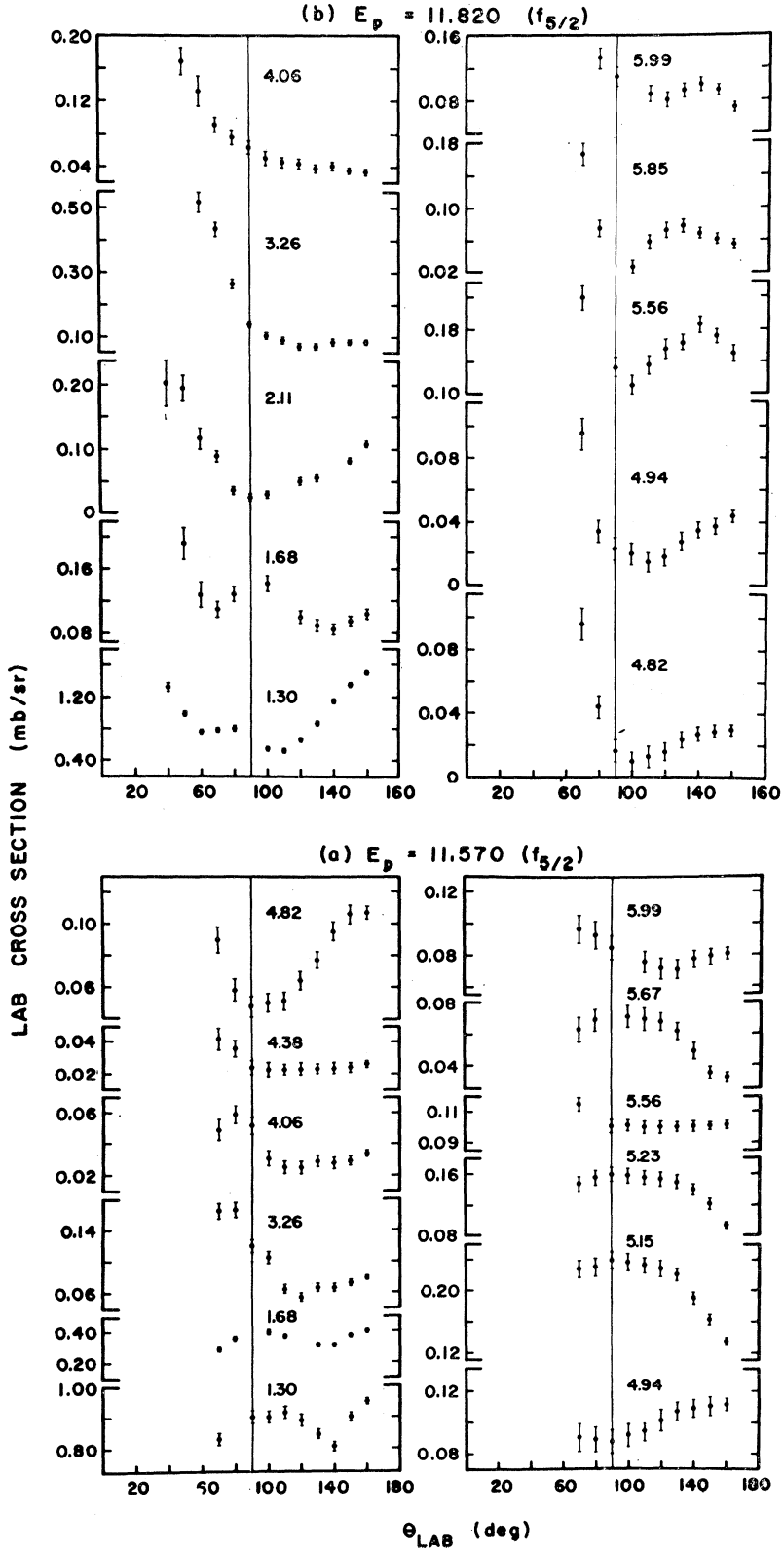

FIG. 7. Inelastic angular distributions for the scattering of protons from ^{136}Xe measured near the first (a) and second (b) $f_{5/2}$ analog resonances.

In addition to the above processes, direct Coulomb or nuclear excitation of 2^+ or 3^- phonon states may be increased (process III) on analog resonances. Finally, there may be increased compound inelastic scattering (process IV) arising from passage through T-lower compound-nuclear states with which the doorway analog state may be mixed. Such a process should resonate in all exit channels at all resonances, and would thus seem to be a small effect relative to the dominant processes. Information on the relative importance of these processes may be obtained from the observed angular distributions as well as from their relative yields on resonance; in particular, mechanisms I, II, and IV should yield symmetric angular distributions.

The most striking characteristic of the angular distribution of the p', 2_1^+ state ($E^*=1.30$ MeV) at the low-lying analog resonances is an increase in the yields at backward angles, resulting in a minimum in the cross section in the neighborhood of 90°. The resonant angular distributions are not symmetric, but much more so than the angular distribution measured at an off-resonance energy [Fig. 5(b)], which displays the strong forward peaking characteristic of a direct interaction process. Since process II is parity forbidden, it would appear that decay of the analog resonances to the 2_1^+ state takes place primarily by process I, with the emission of a p- or f-wave proton. Rather similar behavior is observed in the angular distribution of the second excited state at 1.68-MeV excitation.

The 1.30-MeV state has been previously identified on the basis of systematics as the first 2^+ quadrupole vibration.[12] Since the 1.68-MeV state resonates at the low-lying analog resonances in a way which is similar to the 1.30-MeV state, we believe that it is probably also a collective state.

A notable difference in the yields to the 1.30- and 1.68-MeV states is the presence of a strong resonance in the yield to the 2_1^+, 1.30-MeV state at 11.81 MeV which appears only weakly in the yield to the 1.68-MeV state. On the other hand, a strong resonance appears in the yield to the 1.68-MeV state at approximately 12.1 MeV, which appears weakly or not at all in the yield to the 1.30-MeV level. These selective resonances may be due to "weak-coupling" effects. In the particle-plus-phonon picture, one might see states in ^{137}Xe built by coupling a $f_{7/2}$ neutron to the 2_1^+ state of ^{136}Xe. The centroid of these states should be at approximately $E_x=1.30$ MeV, or for their analogs at $E_p=11.6$ MeV, which is reasonably close to the observed resonance at 11.8 MeV. Similarly, the centroid of analog states whose parent states are formed by coupling a $f_{7/2}$ neutron to the second excited state of ^{136}Xe at 1.68 MeV should be at approximately 11.9 MeV, reasonably close to the observed resonance at 12.1 MeV.

[12] N. R. Johnson and G. D. O'Kelley, Phys. Rev. **114**, 279 (1959).

If we consider the decay of an isobaric analog resonance to the 3^- collective state, process I would be allowed if the parent analog state contains a significant fraction of a neutron coupled to the 3_1^- state of ^{136}Xe to give the correct spin and parity; that is, if the ground-state analog wave function can be written as

$$\psi_0{}^A=[1/(2T_0+1)^{1/2}][T^-\{\alpha(f_{7/2})_n\psi_0\}+T^-\{\beta(l_j)_n\psi_{2^+}\}_{7/2^-}+T^-\{\gamma(l_j)_n\psi_{3^-}\}_{7/2^-}\cdots],$$

where γ is significantly greater than zero. Values of $l=0$ and $l=2$ should contribute to the third term.

Process II can contribute to the decay to the 3_1^- state at the $f_{7/2}$ isobaric analog resonance if 1-particle–1-hole terms of the type $\{(f_{7/2})_n\ (s_{1/2})_n{}^{-1}\psi_0\}_{3^-}$ and $\{(f_{7/2})_n\ (d_{3/2})_n{}^{-1}\psi_0\}_{3^-}$ are present in the 3_1^- wave function. At the $p_{3/2}$ isobaric analog resonance, terms of the type $\{(p_{3/2})_n\ (s_{1/2})_n{}^{-1}\psi_0\}$ cannot couple to 3^-, and at the $p_{1/2}$ analog resonance, neither $\{(p_{1/2})_n\ (s_{1/2})_n{}^{-1}\psi_0\}$ nor $\{(p_{1/2})_n\ (d_{3/2})_n{}^{-1}\psi_0\}$ terms can couple to 3^-.

The identity of the lowest 3^- collective state in ^{136}Xe is uncertain. The 3.26-MeV state is rather puzzling, since it resonates strongly at the $f_{7/2}$ isobaric analog resonance although it is more than 0.50 MeV below the other $(f_{7/2}, j^{-1})$ particle-hole states. The yield to this state gradually increases beyond the $f_{7/2}$ resonance, and its angular distribution, both on and off resonance, displays forward peaking, indicating a direct interaction contribution.

It has been demonstrated[13] that natural parity states tend to have a larger direct interaction contribution than do states of unnatural parity and thus the 3.26-MeV state is probably of natural parity. The best fit for this state, as will be shown in Sec. V B, was obtained with a 3^- assignment. If this state is the lowest 3^- collective state in ^{136}Xe, we expect that its wave function must have a large 1-particle–1-hole component of the type $\{(f_{7/2})_n(s_{1/2})_n{}^{-1}\psi_0\}_{3^-}$ or $\{(f_{7/2})_n\ (d_{3/2})_n{}^{-1}\psi_0\}_{3^-}$. Consequently, decay from the $f_{7/2}$ isobaric analog resonance occurs primarily through process II. Since no further resonances are observed in the yield to this state, any significant contributions from process I are not significant.

We will not attempt to make inferences about the character of the other observed states with excitations below 3.26 MeV; in part because they are obscured by contaminants and in part because their excitation-function behavior is complex. It has been demonstrated that[14] many of the low-lying states in $N=82$ nuclei below 3-MeV excitation can be well described as proton excitations in which the $Z=50$ and $N=82$ shells are closed while the remaining $(Z-50)$ protons are distributed over the next higher major shell. It seems probable that many of the observed states below 3 MeV are proton shell-model states of this type.

[13] C. F. Moore, J. L. Parish, P. von Brentano, and S. A. A. Zaidi, Phys. Letters **22**, 616 (1966).

[14] B. H. Wildenthal (to be published).

TABLE I. Possible spins and parities of the lowest neutron particle-hole states expected in ^{136}Xe at the $f_{7/2}$, $p_{3/2}$, $p_{1/2}$, $f_{5/2}$, and $f_{5/2}$ analog resonances, assuming only $d_{3/2}$ and $s_{1/2}$ hole states are possible. Centroid energies for these states are also indicated.

Configuration	I^π	Centroid energy (MeV)
$f_{7/2}(d_{3/2})^{-1}$	$2^-3^-4^-5^-$	4.11
$f_{7/2}(s_{1/2})^{-1}$	3^-4^-	4.39
$p_{3/2}(d_{3/2})^{-1}$	$0^-1^-2^-3^-$	4.67
$p_{3/2}(s_{1/2})^{-1}$	1^-2^-	4.95
$p_{1/2}(d_{3/2})^{-1}$	1^-2^-	5.02
$p_{1/2}(s_{1/2})^{-1}$	0^-1^-	5.30
$f_{5/2}(d_{3/2})^{-1}$	$1^-2^-3^-4^-$	5.31
$f_{5/2}(s_{1/2})^{-1}$	2^-3^-	5.59
$f_{5/2}(d_{3/2})^{-1}$	$1^-2^-3^-4^-$	5.52
$f_{5/2}(s_{1/2})^{-1}$	2^-3^-	5.80

B. Analysis of Particle-Hole States

We now consider the structure of states with excitations greater than 3.13 MeV. Virtually all these states have excitation functions which resonate at some, but not all, of the analog resonances. We believe that this behavior is indicative of large neutron particle-hole components in the wave functions of these states,[3,4,8] and as a first approximation we shall treat them as neutron particle-hole states. The analysis we present below is essentially empirical and is intended to be only a first approximation. A preliminary account of this analysis has been given previously.[15]

The particle-hole states we will consider are expected to have configurations in which the particle is in a level above $N=82$ ($2f_{7/2}$, $3p_{3/2}$, $3p_{1/2}$, $2f_{5/2}$), and the hole is in a level below $N=82$ ($2d_{3/2}$, $3s_{1/2}$, $1h_{11/2}$, $2d_{5/2}$). In the present analysis the possibility of $h_{11/2}$ or $d_{5/2}$ holes was not considered because of the high angular momentum involved in an $h_{11/2}$ transition and because these two levels lie furthest from the Fermi surface in ^{136}Xe. Particle-hole states were therefore considered to be populated by inelastic emission of a $d_{3/2}$ or $s_{1/2}$ proton from the analog state formed in the reaction.

Table I shows the possible spins and parities of the lowest neutron particle-hole states expected in ^{136}Xe on the basis of these four resonances, assuming only $d_{3/2}$ and $s_{1/2}$ hole states. In some instances, the same spins can arise from several different configurations. The centroid energies expected for these states were obtained by subtracting the neutron binding energy in ^{137}Xe, determined from the ^{136}Xe(d, p) ^{137}Xe analysis,[11] from that in ^{135}Xe, determined from the ^{136}Xe(d, t) ^{135}Xe analysis.[11]

As is evident from the excitation functions shown in Fig. 4, six rather closely spaced states at excitations between 3.78 and 4.38 MeV, as well as one lower state at an excitation of 3.26 MeV, display strong resonant behavior at a laboratory proton energy of 10.270 MeV, corresponding to excitation of the $f_{7/2}$ ground-state analog resonance. Such resonant behavior suggests that each of these states contains the particle-hole configuration ($f_{7/2}$, j^{-1}) in its wave function. In addition, none of these states, except the ones at 4.15 and 4.27 MeV, resonates strongly at any of the remaining analog resonances, indicating that the ($f_{7/2}$, j^{-1}) configuration is dominant in the structure of these states. The states at excitations between 4.45 and 5.10 MeV display strong resonances at a laboratory proton energy of 10.874 MeV, corresponding to excitation of the $p_{3/2}$ analog resonance, thus indicating a strong ($p_{3/2}$, j^{-1}) configuration in the structure of these states. Extending these arguments, configurations of ($p_{1/2}$, j^{-1}) and ($f_{5/2}$, j^{-1}) can be inferred in the structure of the various excited states by the resonant behavior of their respective excitation functions at the $p_{1/2}$ and $f_{5/2}$ resonances.

Since the neutron hole and the emitted proton are in the same shell-model states, the angular momentum j of the neutron hole can in principle be determined by analysis of the proton inelastic on-resonance angular distributions. This analysis will also yield information concerning the spin of excited states populated in the reaction.

The theoretical expression used in our analysis[16] is derived from the R-matrix theory as developed by Lane and Thomas.[17] We assume that the single-level approximation is valid and further that the background matrix R_0L_0 is zero. This second assumption is equivalent to the assumption that on resonance, the direct contribution to the inelastic cross section may be neglected in comparison to the compound contribution. This assumption is only partially justified since there is a small but clearly present off-resonance yield in the inelastic excitation functions. We justify this assumption on the basis that our fits at backward angles are reasonably good and that, to our knowledge, no theory which properly takes account of the direct contribution is available. In order to facilitate computation, we have used the J-J coupling scheme[18] instead of the usual L-S coupling scheme. We have also replaced the hard-sphere phase usually found in R-matrix formulas with a corresponding phase calculated with an optical potential.

For the case of inelastic scattering of protons from spin-zero targets at angle θ and bombarding energy E,

[15] P. A. Moore, P. J. Riley, C. M. Jones, M. D. Mancusi, and J. L. Foster, Phys. Rev. Letters **22,** 356 (1969).

[16] A similar expression has been given previously by S. A. A. Zaidi, P. von Brentano, K. Melchior, P. Rauser, and J. P. Wurm, in *Isobaric Spin in Nuclear Physics*, edited by J. D. Fox and D. Robson (Academic Press Inc., New York, 1968), p. 798.

[17] A. M. Lane and R. G. Thomas, Rev. Mod. Phys. **30,** 257 (1958).

[18] D. D. Long and J. D. Fox, Phys. Rev. **167,** 1131 (1968).

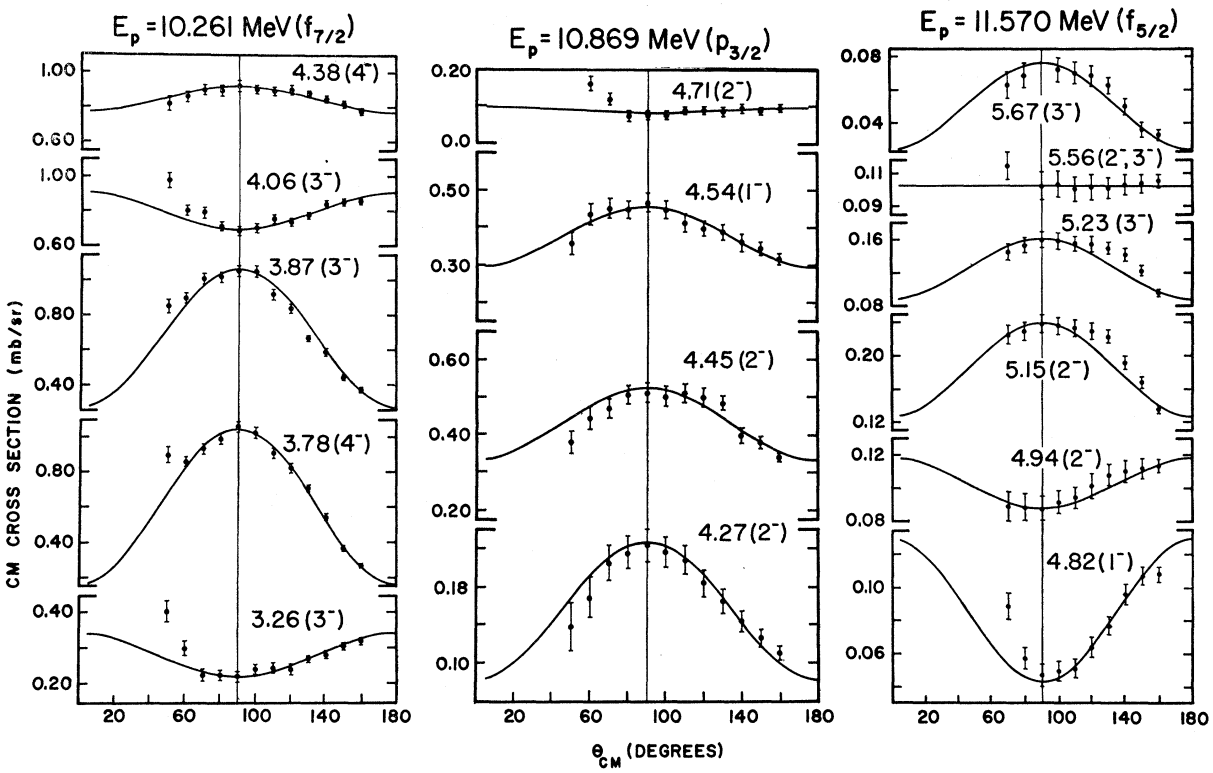

FIG. 8. Fits, indicated by the solid lines, to ^{136}Xe(p, p')^{136}Xe angular distributions at the (a) $f_{7/2}$, (b) $p_{3/2}$, and (c) first $f_{5/2}$ isobaric analog resonances, corresponding to center-of-mass proton energies of 10.186, 10.790, and 11.486 MeV, respectively. The excitation energy of the residual state and assumed spin value (in parentheses) are indicated. The fit shown for the 5.56-MeV state is the same for both of the spin values indicated.

our expression is

$$\sigma(\theta)=\frac{\lambda^2\Gamma_p}{2}\frac{(2J+1)(-)^{2J-I}}{4(E-E_\gamma)^2+\Gamma^2}\sum_{\lambda=0}^{2J-1}P_\lambda(\cos\theta)\bar{Z}(LJLJ;\tfrac{1}{2}\lambda)\times\sum_{j_1j_2}\cos(\xi_{j_1}-\xi_{j_2})\times(\pm\Gamma_{Ij_1J}{}^{1/2})(\pm\Gamma_{Ij_2J}{}^{1/2})\bar{Z}(l_1j_1l_2j_2;\tfrac{1}{2}\lambda)W(j_1Jj_2J;I\lambda),$$

where E_r, Γ_p, Γ, J, and L are, respectively, the resonant energy, proton elastic partial width, total width, spin, and orbital angular momentum of the analog state as obtained from fits to the elastic-scattering data. The spin and orbital angular momentum of a given hole state are j_1 and l_1, respectively, while I is the spin of the residual nucleus. The phases ξ_j are given by

$$\xi_j=\delta_{lj}+\sigma_{lj},$$

where δ_{lj} and σ_{lj} are the nuclear and Coulomb phase shifts, respectively, for proton elastic scattering from the appropriate particle-hole excited state of the core at the emission energy of the inelastic protons. These phase shifts were calculated by code GPMAIN[19] using the optical potential deduced from our previous study of elastic scattering from the ground state of the core.[7]

[19] S. A. A. Zaidi (private communication).

Γ_{IjJ} are the inelastic partial proton widths, and were the only free parameters in the data analysis.

In order to calculate spectroscopic factors, it was necessary to estimate single-particle widths $\Gamma_{IjJ}{}^{(sp)}$ corresponding to the observed transitions. These were approximately determined by evaluating the elastic proton partial width of the isobaric analog of a single neutron state of spin j and orbital angular momentum lying below the observed analog state by an energy equal to the excitation energy of the final state. This width is given by the equation[20]

$$\Gamma_{IjJ}{}^{(sp)}=\Gamma_{lj}{}^{(sp)}=(k'T_0/E_p')\,|\,\langle\varphi_{nA}\,|\,V_1\,|\,X_{pC}{}^{(+)}\rangle\,|^2,$$

and was evaluated using code GPMAIN. E_p' is the emission energy of the inelastic protons. The proton inelastic spectroscopic factors were evaluated from

$$S_{pp'}(j)=\Gamma_{IjJ}(2J+1)/\Gamma_{IjJ}{}^{(sp)}(2I+1).$$

For a given particle-hole state, the relative magnitude of $S_{pp'}$ $(\frac{3}{2})$ and $S_{pp'}$ $(\frac{1}{2})$ determines the strength of the $s_{1/2}$ and $d_{3/2}$ holes in the configuration of the state.

[20] S. A. A. Zaidi and S. Darmodjo, Phys. Rev. Letters **19**, 1446 (1967).

If we consider the $f_{7/2}$ resonance, it is apparent from Table I that states with a final spin of 2^- or 5^- must have a pure $(f_{7/2}, d_{3/2}^{-1})$ particle-hole configuration, with no $s_{1/2}$ contribution allowed. Theoretical angular distributions for these two final spins therefore have a unique shape characteristic of the final spin value. On the other hand, states with a final spin 3^- or 4^- may be formed by a pure $(f_{7/2}, d_{3/2}^{-1})$ configuration, by a pure $(f_{7/2}, s_{1/2}^{-1})$ configuration, or by an admixture of these two hole states. The degree of this admixture is determined by the relative magnitude of the $s_{1/2}$ and $d_{3/2}$ inelastic partial widths. It is possible to obtain a wide range of shapes for the theoretical angular distribution corresponding to a single final spin and consequently it is often possible to obtain a good fit to the experimental angular distribution for more than one final spin value Thus, in general, it is necessary to use the resonant behavior of the inelastic excitation functions for a given state in conjunction with the shape of its experimental angular distribution to determine its final spin.

Fits to the experimental angular distributions at the $f_{7/2}$, $p_{3/2}$, and first $f_{5/2}$ analog resonances, for those states whose excitation functions exhibit the characteristic particle-hole behavior and for which we were able to obtain good experimental angular distributions, are shown in Fig. 8. In the cases where more than one particle component is present, we have analyzed only the angular distribution at the most pronounced resonance. These predictions are for the final spin values, indicated in the figure, which were considered to be the most probable assignments in each case. No fits were attempted for the second $f_{5/2}$ resonance, partly because of the lack of strong particle-hole states on this resonance, but also because problems with high background made it difficult to obtain accurate cross sections on this resonance for those states which do exhibit some resonant behavior. Nor was any attempt made to fit the $p_{1/2}$ resonance angular distributions since the theory predicts isotropic angular distributions in every case for a $p_{1/2}$ particle configuration. At this resonance, only the 4.71-, 4.82-, and 4.94-MeV states display significant resonant behavior, and of these only the 4.82-MeV angular distribution is clearly anisotropic at backward angles.

Fits were made at the $f_{7/2}$ resonance for all observed particle-hole states except the ones at 4.15 and 4.27 MeV. These two states could not be fit due to the asymmetry of their angular distributions, though their spins are limited to values of 2^- or 3^- by their resonant behavior. The state at 4.27 MeV was fit on the $p_{3/2}$ resonance and will be discussed later. The shape of the 4.15-MeV state angular distribution indicates that the spin of this state is probably 2^- (and not 3^-). Angular distributions for the states at 3.78 and 3.87 MeV are symmetric [indicating a predominant $(f_{7/2}, d_{3/2}^{-1})$ configuration with a slight $(f_{7/2}, s_{1/2}^{-1})$ admixture], strongly anisotropic, and could both be fit with either 3^- or 4^- spin assignments. It is possible that the assignments shown in Fig. 8 for these two states should be reversed. The states at excitations of 4.06 and 4.38 MeV are nearly isotropic [indicating a predominant $(f_{7/2}, s_{1/2}^{-1})$ configuration with a slight $(f_{7/2}, d_{3/2}^{-1})$ admixture], and also could both be fit with either a 3^- or a 4^- assignment. The 4.06-MeV state must be a 3^- state, however, since its excitation function resonates slightly at the $p_{3/2}$ resonance. In addition, the angular distribution for this state displays a slight forward peaking and the yield to this state tends to increase slightly with increasing bombarding energy, indicating a certain amount of direct interaction contribution to the cross section. As mentioned above, it has been demonstrated[13] that natural parity states tend to have a larger direct interaction contribution to their cross section than do states of unnatural parity, indicating a spin assignment of 3^- for the 4.06-MeV state. The 4.38-MeV state exhibits none of these tendencies and is probably of unnatural parity, consistent with a 4^- spin assignment. The 3.26-MeV state, which occurs more than 0.50 MeV below the other $(f_{7/2}, j^{-1})$ states, has been discussed previously. The best fit for this state was obtained with a 3^- assignment, though its angular distribution could also be fit with an assignment of 5^-.

At the $p_{3/2}$ resonance, it was not possible to obtain fits for the states at 4.15 and 5.10 MeV. Qualitative arguments, however, based on the resonant behavior of these two states, indicate a probable spin assignment of 2^- for each state. Fits of equal quality can be obtained for the 4.27-MeV state with either a 1^- or a 2^- final spin, but a spin of 2^- must be assigned because this state resonates on the $f_{7/2}$ analog resonance. Both the state at 4.45 MeV and that at 4.54 MeV can be fit by final spins of 1^- and 2^-, and it is by no means clear which of these spins is correct. The fits shown for these states correspond to the best value of X^2 obtained for the two possible spin assignments for each of these states. The 4.71-MeV state could be fit equally well with assignments of 1^-, 2^-, or 3^-, but the resonant behavior of the excitation function for this state eliminates the 1^- and 3^- assignments. The 4.71-MeV state is assigned a spin of 2^- on this basis.

Of the ten states displaying significant resonances indicative of a particle-hole configuration at the first $f_{5/2}$ analog resonance, it was possible to obtain fits for the six states shown in Fig. 8(c). The 4.94-MeV state was limited, by its resonant behavior, to spin assignments of 1^- and 2^-. A fit could, however, be obtained only for the 2^- assignment, and the 4.94-MeV state was assigned this spin. For the 4.82-MeV state, on the other hand, fits were possible using both spins (1^- and 2^-) allowed by its resonant behavior. The 1^- assignment is considered to be correct, however, due to the better quality of the fit for this spin, and due to the fact that the theoretical shape for this spin value is unique since no $s_{1/2}$ admixture is allowed. The 5.56-MeV state is apparently isotropic and probably corresponds very

TABLE II. Particle-hole configurations, inferred final spin values, partial widths, and spectroscopic factors of excited states of ^{136}Xe. In this table, E^* is the excitation of the excited state in ^{136}Xe. The notation j^{-1} for a hole configuration indicates that resonant behavior was observed but that an assignment of relative hole strength was not made. Parentheses indicate small hole-configuration admixtures. Entries under I^π are spins of the residual excited state compatible with fits to the angular distributions and excitation-function behavior. The spin values used in the calculations are underlined. Parentheses indicate that a spin assignment has low probability. Where two spins are given without parentheses, either assignment is considered probable. L_J is the particle configuration used for the fits in Fig. 8. $\Gamma_{I\frac{1}{2}J}$ and $\Gamma_{I\frac{3}{2}J}$ are absolute values of the partial laboratory widths used for the fits in Fig. 8. $S_{pp'}(\frac{1}{2})$ and $S_{pp'}(\frac{3}{2})$ are the corresponding proton inelastic spectroscopic factors as defined in the text.

E^* (MeV)	Compound analog resonance $f_{7/2}$	$p_{3/2}$	$p_{1/2}$	$f_{5/2}$	I^π	L_J	$\Gamma_{I\frac{1}{2}J}$ (keV)	$\Gamma_{I\frac{3}{2}J}$ (keV)	$S_{pp'}(\frac{1}{2})$	$S_{pp'}(\frac{3}{2})$
3.26	$fs^{-1}+(fd^{-1})$				3^-, (5^-)	$f_{7/2}$	1.091	0.129	0.07	0.03
3.78	$(fs^{-1})+fd^{-1}$				3^-, 4^-	$f_{7/2}$	1.000	2.500	0.08	0.87
3.87	$(fs^{-1})+fd^{-1}$				3^-, 4^-	$f_{7/2}$	2.110	1.630	0.24	0.81
4.06	$fs^{-1}+(fd^{-1})$	(pd^{-1})			3^-	$f_{7/2}$	3.481	0.106	0.48	0.07
4.15	fd^{-1}	pj^{-1}			2^-, (3^-)					
4.27	fd^{-1}	$(ps^{-1})+pd^{-1}$			2^-	$p_{3/2}$	0.942	0.761	0.06	0.21
4.38	$fs^{-1}+(fd^{-1})$				(3^-), 4^-	$f_{7/2}$	4.000	0.070	0.64	0.05
4.45		$ps^{-1}+pd^{-1}$			1^-, 2^-	$p_{3/2}$	3.771	0.622	0.29	0.21
4.54		$ps^{-1}+pd^{-1}$			1^-, 2^-	$p_{3/2}$	3.642	0.208	0.51	0.13
4.71		$ps^{-1}+pd^{-1}$	pd^{-1}	(fj^{-1})	2^-	$p_{3/2}$	0.734	0.113	0.07	0.06
4.82		pj^{-1}	pj^{-1}	fd^{-1}	1^-, (2^-)	$f_{5/2}$		1.180		0.66
4.94		pj^{-1}	pd^{-1}	$fs^{-1}+fd^{-1}$	2^-	$f_{5/2}$	1.550	0.056	0.14	0.22
5.10	(fd^{-1})	pj^{-1}		fj^{-1}	2^-					
5.15				$(fs^{-1})+fd^{-1}$	2^-, 3^-	$f_{5/2}$	0.180	3.130	0.20	1.60
5.23				$(fs^{-1})+fd^{-1}$	2^-, 3^-	$f_{5/2}$	0.230	2.017	0.21	0.81
5.56				fs^{-1}	2^-, 3^-	$f_{5/2}$	1.680		0.22	
5.67				$(fs^{-1})+fd^{-1}$	2^-, 3^-	$f_{5/2}$	0.596	0.365	0.09	0.27

closely to a pure $s_{1/2}$ hole configuration, though the cross-section prediction for such a case is the same for a 2^- or a 3^- spin assignment. The remaining states, at excitations of 5.15, 5.23, and 5.67 MeV, respectively, were difficult to fit and could be fit with either a 2^- or a 3^- assignment. The fits shown for these states correspond to the smallest value of X^2 obtained in each case.

Particle-hole configurations, inferred final spin values, partial widths, and spectroscopic factors are shown in Table II. The entry of a particle-hole configuration in this table indicates the presence of resonant behavior. Thus, for example, the 4.27-MeV transition resonated at both the $f_{7/2}$ and $p_{3/2}$ compound resonances indicating the presence of both fd^{-1} and (ps^{-1} and pd^{-1}) components in the wave function of the residual state. The relative size of $S_{pp'}(\frac{1}{2})$ and $S_{pp'}(\frac{3}{2})$ indicates the extent of the admixture of the $s_{1/2}$ and $d_{3/2}$ holes for a given particle-hole configuration. The upper limit of unity on the spectroscopic factors is exceeded, for the most probable spins, only in the case of the 5.15-MeV state. The sums of the $d_{3/2}$ and $s_{1/2}$ spectroscopic factors at the $f_{7/2}$ resonance are 1.83 and 1.51, respectively. The sum rule

$$\sum_i S_{pp'}{}^{(i)}(Jj) = 2j+1,$$

where j is the spin of the hole state, indicates that the sum of the $d_{3/2}$ spectroscopic factors should be 4.00, and that of the $s_{1/2}$ spectroscopic factors, 2.00. Only about one-half of the total $d_{3/2}$ hole strength is accounted for, as is expected, since only 3^- and 4^- spins have been analyzed at this resonance, and $d_{3/2}$ strength will be present in 2^- and 5^- states. The $s_{1/2}$ sum rule is, as expected, nearly satisfied. The situation is more complicated at the $p_{3/2}$ and $f_{5/2}$ resonances since at the $p_{3/2}$ resonance the data allowed analysis of only four out of nine particle-hole states, and at the $f_{5/2}$ resonance, only six out of ten particle-hole states.

VI. SUMMARY AND CONCLUSIONS

Thirty-six excited states at excitations between 1.30 and 6.29 MeV have been identified and their Q value determined in proton inelastic scattering from ^{136}Xe. Excitation functions for 34 of the excited states have been obtained for laboratory proton energies between 9.77 and 12.98 MeV. The 2^+ first excited state at 1.30 MeV and the next eight low-lying states up to approximately 3 MeV in excitation resonate strongly at many of the analog resonances. The dominant contribution to the resonant behavior of these states is probably related to the existence of significant components of low-lying excited-state wave functions in the core wave function. Some evidence for core-coupled resonances in these low-lying excited states is observed. Excitation functions for many of the remaining states above 3-MeV excitation exhibit a resonant behavior which indicates that these states can be described as neutron-particle–neutron-hole states. The particle configuration of these states was determined by an examination of their ex-

citation functions. Inelastic angular distributions for the particle-hole states at the $f_{7/2}$, $p_{3/2}$, and first $f_{5/2}$ analog resonances were fit with a single-level R-matrix formula expressed in a j-j coupling scheme in order to determine hole configurations, assuming that only $s_{1/2}$ and $d_{3/2}$ holes are involved. Proton inelastic partial widths determined from the fits were used to calculate $s_{1/2}$ and $d_{3/2}$ spectroscopic factors for the particle-hole states, the degree of admixture of the hole configuration in the structure of a given state being determined by the relative magnitude of the respective $s_{1/2}$ and $d_{3/2}$ spectroscopic factors. Using the results of this analysis in conjunction with the resonant behavior of the corresponding inelastic excitation functions, it was possible to determine the particle-hole configurations and probable final spin assignments for 17 particle-hole excited states in ^{136}Xe.

ACKNOWLEDGMENTS

The data reported in this work were taken at Oak Ridge National Laboratory, and we wish to thank the members of the Laboratory for their cooperation and help during the experiment. The authors are indebted to Dr. S. A. A. Zaidi for helpful discussions and assistance in carrying out the analysis. One of us (P.A.M.) gratefully acknowledges financial support from an Atomic Energy Commission Special Fellowship in Nuclear Science and Engineering.

PHYSICAL REVIEW C VOLUME 1, NUMBER 3 MARCH 1970

Sensitivity of the Half-Life of Nb^{90m} to Chemical Environment*

ARTHUR OLIN†
Lyman Laboratory of Physics, Harvard University, Cambridge, Massachusetts 02138

(Received 30 October 1969)

Changes in the decay constant of the isomer Nb^{90m} were measured. We found that $(\lambda_{\text{Nb (fluoride complex)}}-\lambda_{\text{Nb}})/\lambda_{\text{Nb}}=(-3.9\pm0.8)\times10^{-2}$; $(\lambda_{\text{Nb}_2\text{O}_5}-\lambda_{\text{Nb}})/\lambda_{\text{Nb}}=(-1.9\pm0.5)\times10^{-2}$. The Nb (fluoride complex) result confirms the value previously obtained by Cooper *et al.*, which had been questioned because of the negative result obtained by Weirauch *et al.* in a similar measurement. Some possible causes of this high sensitivity to chemical environment are discussed.

INTRODUCTION

THERE has been recent interest in the sensitivity of the half-life of the 20-sec isomer Nb^{90m} to different chemical environments. This isomer is believed to decay through a highly converted 2.4-keV $M2$ transition, although evidence for this is indirect.[1] This transition is followed by a prompt 122.4-keV $E2$ γ ray (see Fig. 1). The isomeric state is populated by the decay of 5.7-h Mo^{90}, and may be produced directly by the reaction $Zr^{90}(d, 2n)Nb^{90m}$.

Cooper *et al.*[2] have reported a 3.6% increase in the half-life when a niobium foil containing Nb^{90m} is dissolved in a 2:1 mixture of concentrated HF and HNO_3. This is by an order of magnitude the largest change in half-life observed in any isomer. Weirauch *et al.*[3] have measured directly the half-life of Nb^{90m} in Zr metal, and in a fluoride complex produced by dissolving a Zr foil containing Nb^{90m} in a mixture of HF and HNO_3 containing dissolved Nb powder. They were unable to find any difference in the half-life with an experimental error of 1%. One might attribute this discrepancy to the slightly different chemical environment used by each group. However, there was also a difference in the techniques of the various workers.

Motivated by the large environmental sensitivity reported by Cooper *et al.*, we recently measured a small change in the Nb^{90m} half-life induced by superconductivity.[4] In view of Weirauch's measurements, we decided to make an independent check of Cooper's result, taking particular account of source geometry changes due to the source diffusing through the sample volume, and also the possibility of volatile Nb compounds evolving after the reaction. We have also observed a difference in half-life between Nb metal and Nb_2O_5.

METHOD

The change in half-life of the 20-sec isomeric state was measured with the Nb^{90m} in equilibrium with its parent Mo^{90}. This is the method first used by Cooper *et al.*[2] A sudden increase in the Nb^{90m} decay rate will increase the intensity of the 122-keV line; this will decay back with a 20-sec half-life to reestablish radioactive equilibrium with the parent Mo^{90}. If the decay

* Research supported in part by the U.S. Office of Naval Research, under Contract No. Nonr-1866 (56) with Harvard University.

† National Research Council of Canada Scholar.

[1] J. A. Cooper, J. M. Hollander, and J. O. Rasmussen, Nucl. Phys. **A109**, 603 (1968).

[2] J. A. Cooper, J. M. Hollander, and J. O. Rasmussen, Phys. Rev. Letters **15**, 683 (1965).

[3] W. Weirauch, W. D. Schmitt-Ott, F. Smend, and A. Flammersfeld, Z. Physik **209**, 289 (1968).

[4] A. Olin and K. T. Bainbridge, Phys. Rev. **179**, 450 (1969).